BOX 3.2 *(continued)*

direct contact with other pentamers (e.g., Fig. 3.6A), but when $h = 1$ and $k = 1$, each pentamer is separated from neighboring pentamers by one hexamer (Fig. 3.6B). The values of h and k are therefore determined by inspection of electron micrographs of virus particles or their constituents (D). For example, in the phage p22 capsid (top), one pentamer is separated from another by two steps (from one structural unit to the next) along the h axis and one step along the k axis, as illustrated for the bottom left pentamer shown. Hence, $h = 2$, $k = 1$, and $T = h^2 + hk + k^2 = 7$. In contrast, pentamers of the herpes simplex virus type 1 (HSV-1) nucleocapsid (bottom) are separated by four and zero steps, respectively, in the directions of the h and k axes. Thus, $h = 4$, $k = 0$, and $T = 16$. Cryoelectron micrographs of phage P22 and herpes simplex virus type 1 courtesy of B. V. V. Prasad and W. Chiu (Baylor College of Medicine), respectively. (A and B) Adapted from Fig. 2 of J. E. Johnson and A. J. Fisher, *in* R. G. Webster and A. Granoff (ed.), *Encyclopedia of Virology*, 3rd ed. (Academic Press, London, England, 1994), with permission. (C) Adapted from S. Casjens, *in* S. Casjens (ed.), *Virus Structure and Assembly* (Jones and Bartlett Publishers, Inc., Boston, Mass., 1985), with permission.

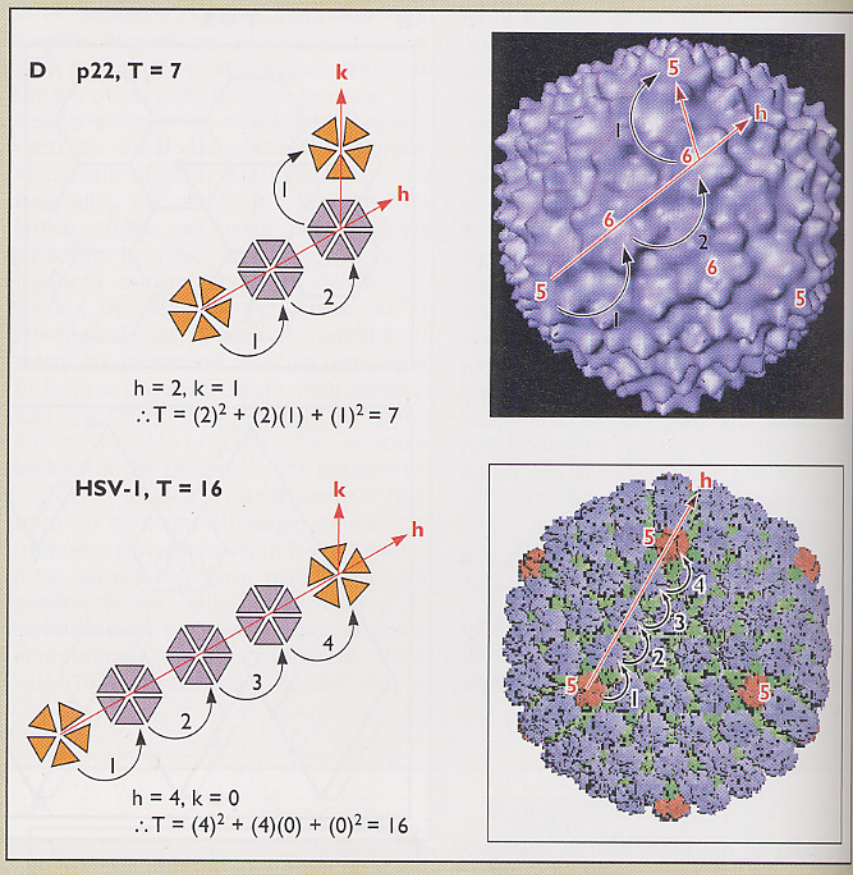

strand RNA viruses, such as tomato bushy stunt virus and black beetle virus, a property that was entirely unanticipated. Even more remarkably, this relationship is not restricted to small RNA viruses: the major capsid proteins of the DNA-containing papovaviruses and adenoviruses al contain such β-barrel domains (see below). One of th most important principles established by high-resolutio structural studies of proteins is the ability of proteins wi

Table 3.3 *T* numbers of representative viruses

Triangulation number (T)[a]	Family	Member(s)	60T	Protein(s) that forms the capsid or nucleocapsid shell
1	*Parvoviridae*	Canine parvovirus	60	60 copies of VP2
3	*Nodaviridae*	Black beetle virus	180	180 copies of coat protein
Pseudo-3	*Picornaviridae*	Poliovirus, human rhinovirus	180	60 copies each of VP1, VP2, VP3, and VP4
4	*Alphaviridae*	Ross River virus	240	240 copies of C protein
7	*Papovaviridae*	Simian virus 40, polyomavirus	420	360 copies of VP1
13	*Reoviridae*	Reovirus, outer shell	780	60 copies of λ2, 600 copies of μ1
16	*Herpesviridae*	Herpes simplex virus type 1	960	960 copies of VP5
25	*Adenoviridae*	Adenovirus type 2	1,500	720 copies of protein II, 60 copies of protein I
189–217	*Iridoviridae*	Ranavirus	11,340; 13,020	?

[a]The triangulation number, T, is a description of the face of an icosahedron indicating the number of equilateral triangles into which each face is divided followi the laws of solid geometry (Box 3.2). The total number of subunits is equal to $60T$ because a minimum of 60 subunits is required to form a closed shell with icos hedral symmetry. Thus, the simplest assembly is $T = 1$. A $T = 3$ icosahedron requires 180 subunits in sets of three; a $T = 4$ icosahedron requires 240 subunits; a T 7 icosahedron requires 420 subunits; and so forth. The 60 structural units of picornavirus capsids each contain four different polypeptides (VP1, VP2, VP3, and VP4 Hence the capsid is described as a pseudo $T = 3$ structure. Note that papovaviruses, reoviruses, and adenoviruses do not contain the number of subunits predicte

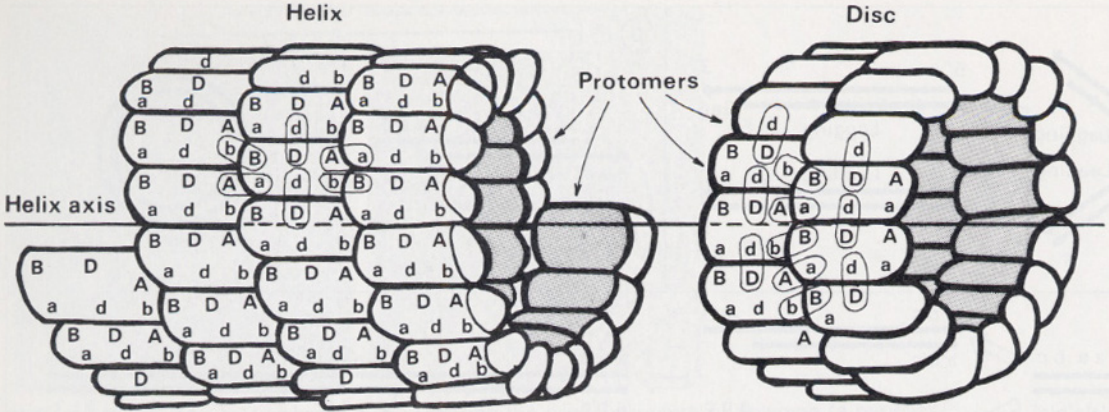

FIG. 46-9. Constitution of the helical capsid. All protomers are identical and establish regularly repeated bonds with their neighbors between chemical groups indicated by **letters**. Since each protomer is staggered in respect to its lateral neighbors, it forms bonds with the two of them on each side along the helix axes. This confers considerable stability on the capsid. The protomers assemble first to constitute flat nonhelical discs containing two rings of protomers, with the staggered arrangement found in the finished helix. Under physiologic conditions when the protomers of the discs associate with the RNA they shift slightly to produce a helix. The helix grows in length by the addition and assimilation of discs.

FIG. 46-12. Electron micrograph of GAL virus (chicken adenovirus) by negative staining, showing capsomer structure. The **arrowed** capsomers are situated on the fivefold axes. (Wildly P, Watson JD: Cold Spring Harbor Symp Quant Biol 27:25, 1962)

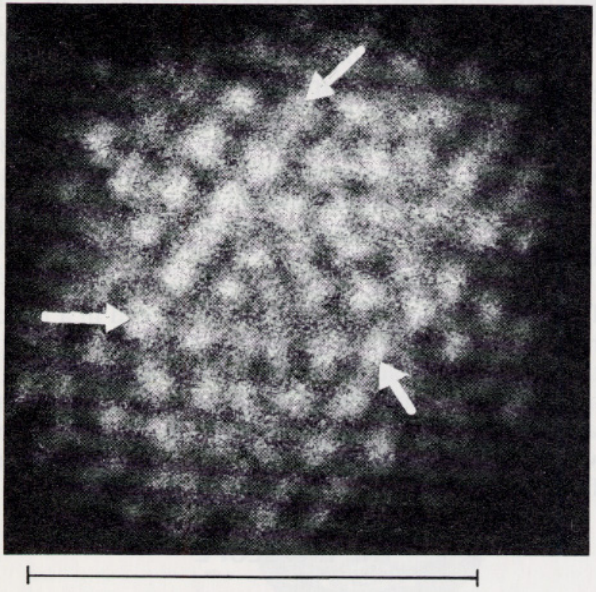

FIG. 46-13. Possible constitution of capsomers from protomers. In the icosahedral capsids, the protomers constitute oligomers of either five or six protomers, called capsomers, which are drawn as seen from the outside of a virion. Every protomer in a capsomer establishes bonds with two neighboring protomers, always through the same chemical groups (diagrammatically indicated as **A–a** and **B–b** in the hexon, and **c–C** and **d–D** in the penton). Each protomer also has other contacts with neighboring capsomers in the complete capsid.

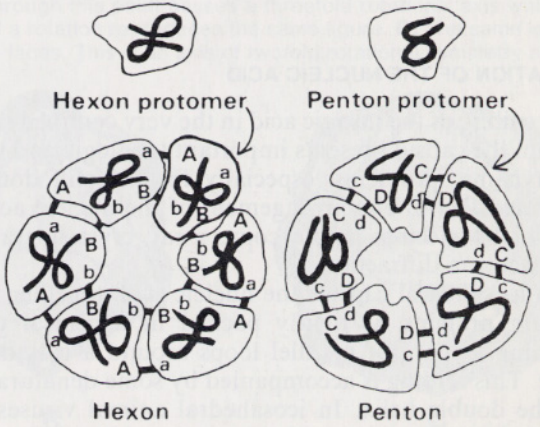

FIG. 46-16. Rotational axes in the icosahedron. The edges of the icosahedron, which limit the triangular faces, are drawn as **heavy lines**. The outlines of the capsomers are in **thin lines**. Pentons are **crosshatched. A.** The icosahedron of Figure 46-15 is viewed looking down the center of a pentagonal capsomer which corresponds to the corner of the polyhedron. Rotating the figures by 1/5 of a rotation reproduces the same figure. A fivefold rotational axis, therefore, passes through the center of the pentagonal capsomer. **B.** The same icosahedron viewed looking down the center of a triangular face. Through this point passes a threefold rotational axis which is situated between three hexagonal capsomers; rotating the figure by 1/3 of a rotation reproduces the same figure. **C.** The same icosahedron viewed looking down the middle of an edge between two triangular faces. This is an axis of twofold rotational symmetry and is situated in the center of a hexagonal capsomer.

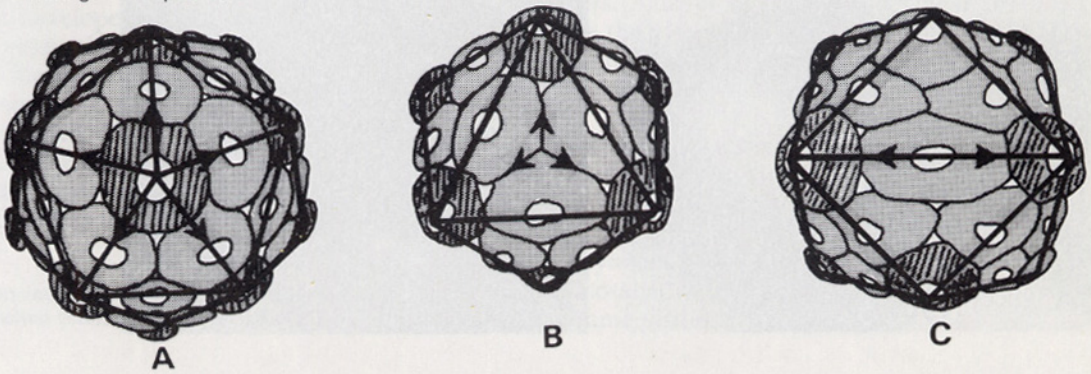

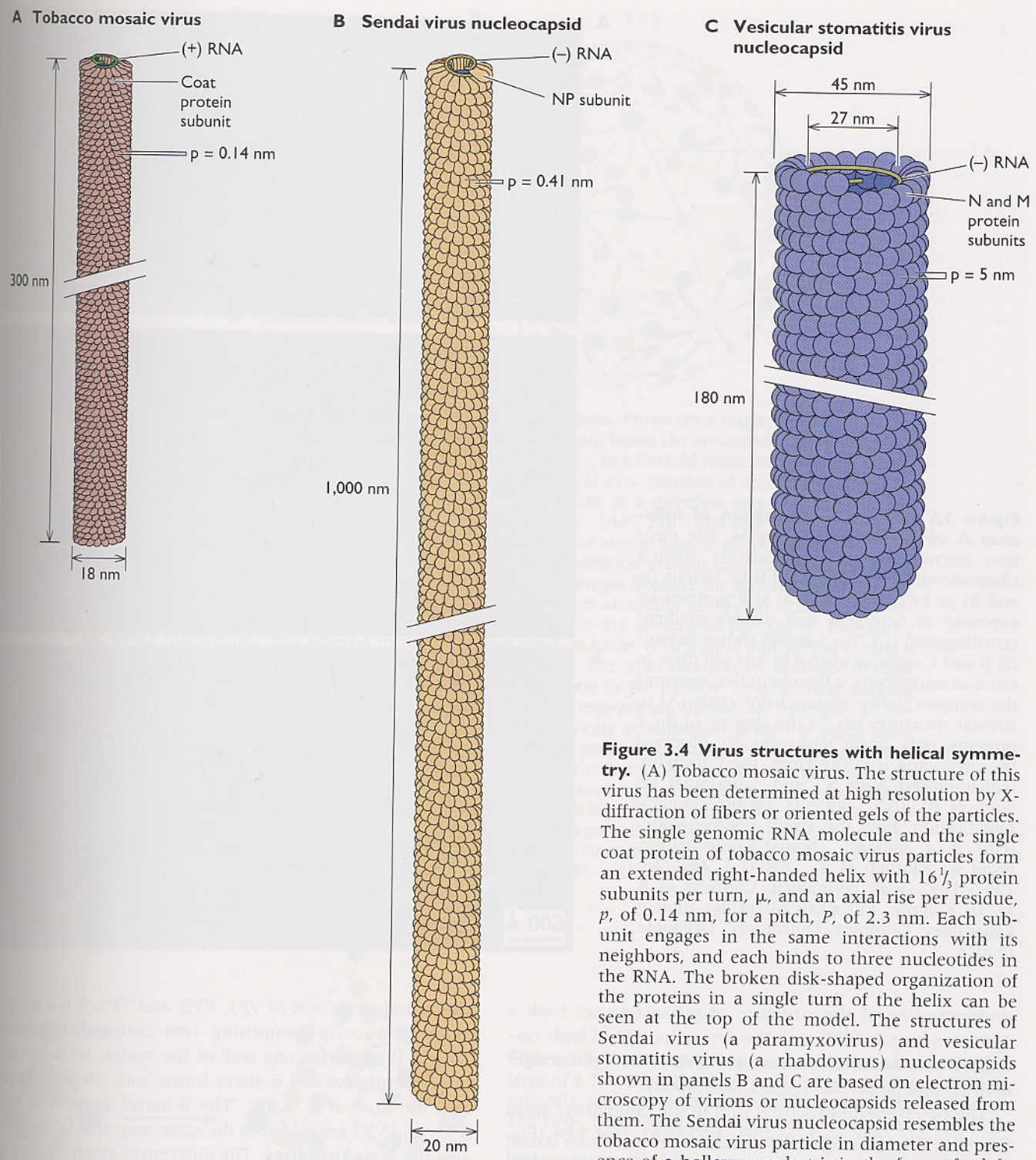

Figure 3.4 Virus structures with helical symmetry. (A) Tobacco mosaic virus. The structure of this virus has been determined at high resolution by X-diffraction of fibers or oriented gels of the particles. The single genomic RNA molecule and the single coat protein of tobacco mosaic virus particles form an extended right-handed helix with $16^{1}/_{3}$ protein subunits per turn, μ, and an axial rise per residue, p, of 0.14 nm, for a pitch, P, of 2.3 nm. Each subunit engages in the same interactions with its neighbors, and each binds to three nucleotides in the RNA. The broken disk-shaped organization of the proteins in a single turn of the helix can be seen at the top of the model. The structures of Sendai virus (a paramyxovirus) and vesicular stomatitis virus (a rhabdovirus) nucleocapsids shown in panels B and C are based on electron microscopy of virions or nucleocapsids released from them. The Sendai virus nucleocapsid resembles the tobacco mosaic virus particle in diameter and presence of a hollow core but is in the form of a left-handed helix with distinctive helical parameters (μ = 13, p = 0.41 nm, P = 5.3 nm). The vesicular stomatitis virus nucleocapsid is also hollow and comprises about 30 turns of uniform diameter, followed by 5 or 6 turns of decreasing diameter. Helical parameters have not been determined.

TABLE 3. *Families containing human and animal viruses*

Virus Family	Characteristics
RNA viruses	
Picornaviridae *Caliciviridae* *Astroviridae*	Single-stranded RNA positive-sense nonsegmented nonenveloped
Togaviridae *Flaviviridae*	Single-stranded RNA positive-sense nonsegmented enveloped
Coronaviridae Floating genus: *Arterivirus*	Single-stranded RNA positive-sense nonsegmented enveloped nested set transcription
Order: *Mononegavirales* *Paramyxoviridae* *Rhabdoviridae* *Filoviridae*	Single-stranded RNA negative-sense nonsegmented enveloped
Orthomyxoviridae *Bunyaviridae* *Arenaviridae*	Single-stranded RNA negative-sense (some ambisense genes) segmented enveloped
Reoviridae *Birnaviridae*	Double-stranded RNA positive-sense segmented nonenveloped
Retroviridae	Single-stranded RNA positive-sense retroid DNA step in replication
DNA viruses	
Hepadnaviridae	Double-stranded/ single-stranded DNA enveloped retroid DNA step in replication
Circoviridae *Parvoviridae*	Single-stranded DNA nonenveloped
Papovaviridae *Adenoviridae*	Double-stranded DNA nonenveloped
Herpesviridae *Poxviridae* *Iridoviridae* Family: unnamed, African swine fever virus	Double-stranded DNA enveloped
Subviral agents: Satellites, Viroids, and Agents of Spongiform Encephalopathies (Prions)	
floating genus: *Deltavirus*	Single-stranded RNA negative-sense nonsegmented defective, satellite
taxon: undefined, unnamed agents of spongiform encephalopathies (prions)	No known nucleic acid prions, "self-replicating" proteins

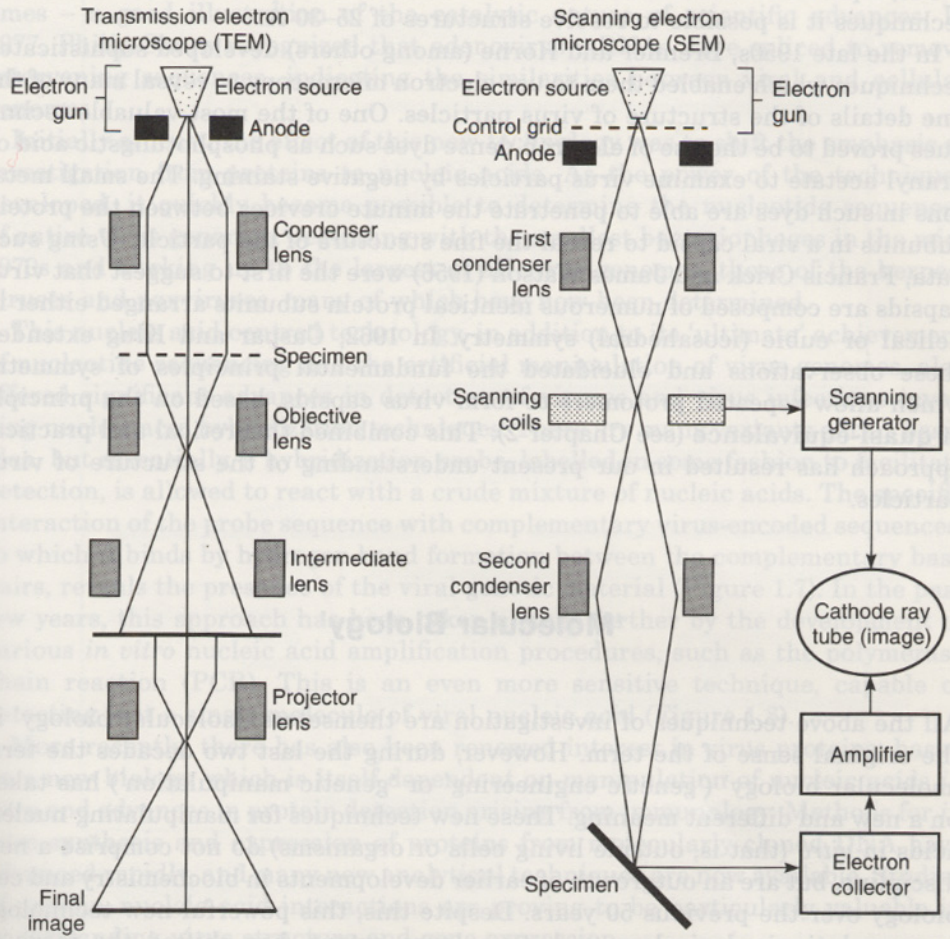

Figure 1.6 Working principles of transmission and scanning electron microscopes.

specific technique, known as immunoelectron microscopy, is gaining ground as a rapid method for diagnosis.

In recent years, developments in electron microscopy have allowed investigation of the structure of fragile viruses which cannot be determined by X-ray crystallography. These include: cryo-electron microscopy, in which the virus particles are maintained at very low temperatures on cooled specimen stages; examination of particles embedded in vitreous ice, which does not disrupt the particles by the formation of ice crystals; low-irradiation electron microscopy, reducing the destructive bombardment of the specimen with electrons; and sophisticated image-analysis and image-reconstruction techniques which permit accurate, three-dimensional images to be formed from multiple images that individually would appear as very poor quality. Conventional electron microscopy can resolve structures down to 50–70 Å in size (a typical atomic diameter is

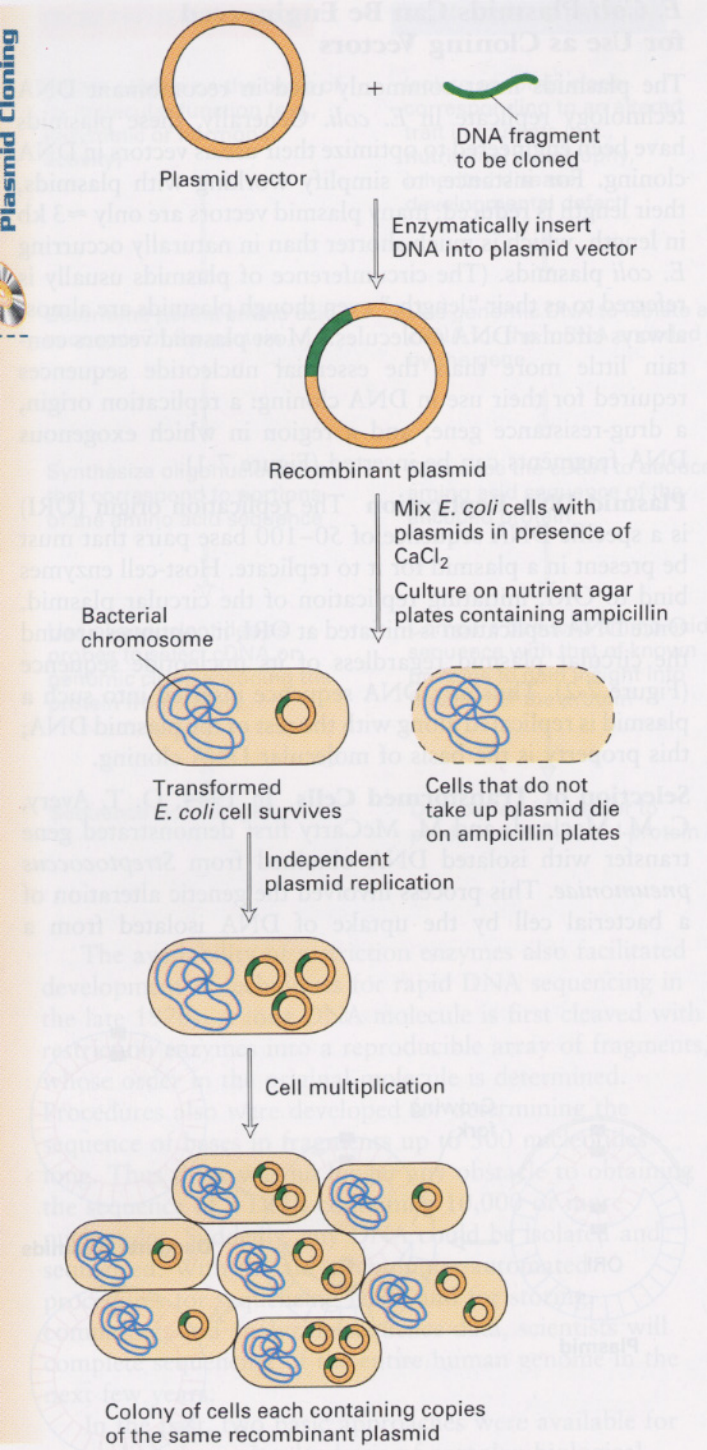
Plasmid vector
+
DNA fragment to be cloned
Enzymatically insert DNA into plasmid vector
Recombinant plasmid
Mix E. coli cells with plasmids in presence of $CaCl_2$
Culture on nutrient agar plates containing ampicillin
Bacterial chromosome
Transformed E. coli cell survives
Cells that do not take up plasmid die on ampicillin plates
Independent plasmid replication
Cell multiplication
Colony of cells each containing copies of the same recombinant plasmid

Figure 2.16

Filter hybridization establishes whether a solution of denatured DNA (or RNA) contains sequences complementary to the strands immobilized on the filter.

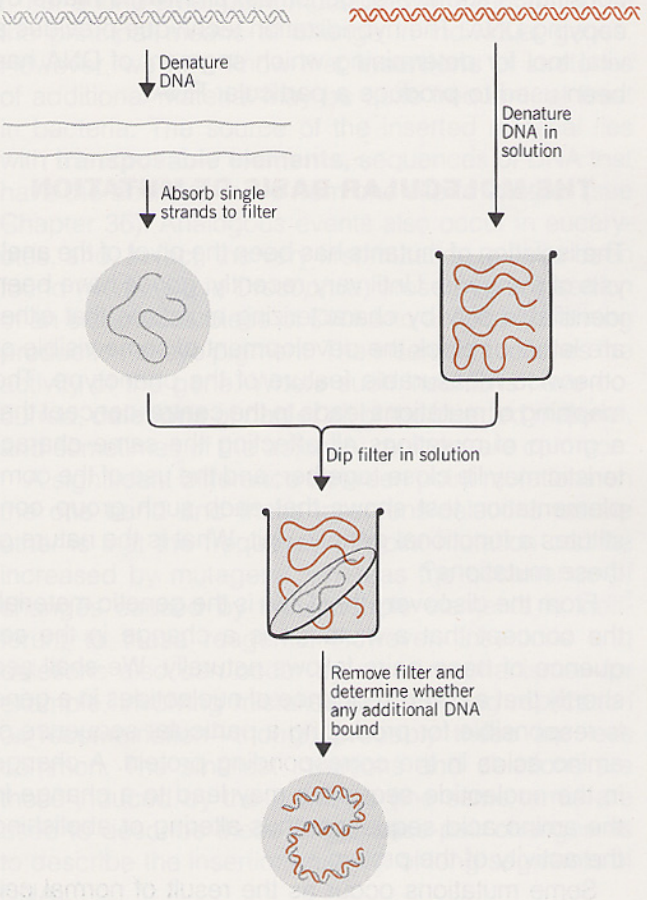

CHAPTER 15
The Polymerase Chain Reaction

INTRODUCTION

The polymerase chain reaction (PCR) is a rapid procedure for in vitro enzymatic amplification of a specific segment of DNA. Like molecular cloning, PCR has spawned a multitude of experiments that were previously impossible. The number of applications of PCR seems infinite—and is still growing. They include direct cloning from genomic DNA or cDNA, in vitro mutagenesis and engineering of DNA, genetic fingerprinting of forensic samples, assays for the presence of infectious agents, prenatal diagnosis of genetic diseases, analysis of allelic sequence variations, analysis of RNA transcript structure, genomic footprinting, and direct nucleotide sequencing of genomic DNA and cDNA.

The theoretical basis of PCR is outlined in Figure 15.0.1. There are three nucleic acid segments: the segment of double-stranded DNA to be amplified and two single-stranded oligonucleotide primers flanking it. Additionally, there is a protein component (a DNA polymerase), appropriate deoxyribonucleoside triphosphates (dNTPs), a buffer, and salts.

The primers are added in vast excess compared to the DNA to be amplified. They hybridize to opposite strands of the DNA and are oriented with their 3′ ends facing each

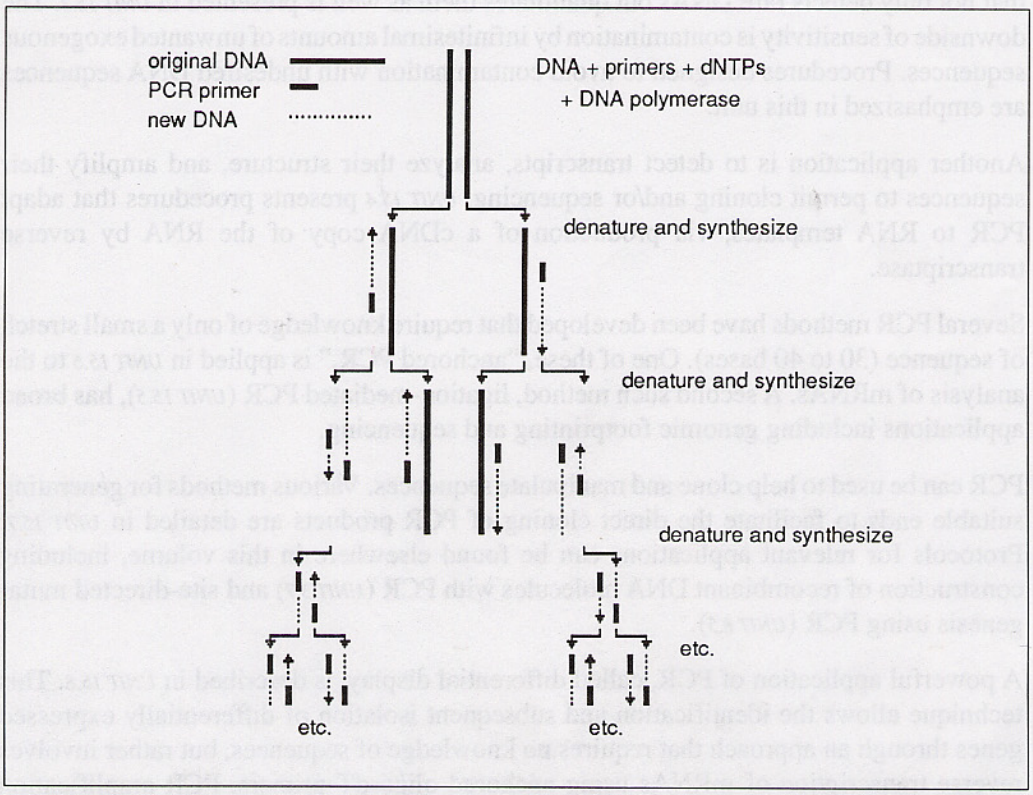

Figure 15.0.1 The polymerase chain reaction. DNA to be amplified is denatured by heating the sample. In the presence of DNA polymerase and excess dNTPs, oligonucleotides that hybridize specifically to the target sequence can prime new DNA synthesis. The first cycle is characterized by a product of indeterminate length; however, the second cycle produces the discrete "short product" which accumulates exponentially with each successive round of amplification. This can lead to the many million-fold amplification of the discrete fragment over the course of 20 to 30 cycles.